Remote Extinction of a 2.4 GHz RF Front-End Using Millimeter-Wave EMI in the Near-Field

Pierre Payet, Jérémy Raoult, and Laurent Chusseau

Abstract—The effects of highly out-of-band electromagnetic interference (EMI) on an RF front-end are experimentally evaluated. Irradiation at 60 GHz with a moderate power is produced in the near-field owing to an open-ended WR15 waveguide fed by a Gunn diode. Surprisingly, we easily obtain the remote extinction of either the transmitter or the receiver of the front-end subject to EMI. The paper proposes a detailed analysis of both CW and chopped EMI by varying almost all experimental conditions, namely the polarization, target distance, and chopping mode. The latter shows most efficiency and evidences some long time scale dynamics in the induced perturbation.

1. INTRODUCTION

The electronic immunity of integrated circuits (IC) is of major concern with the increasing density of components and systems able to communicate [1]. Such disturbances are usually considered within the nominal operating bandwidth where it is feared that they are the most dangerous. But out-of-band investigations have to be performed since the intrinsic performances of the individual active components are often much higher than the designed IC frequency of operation. This must be considered with both analog and digital circuits.

In [2], digital circuits of clock frequencies in the MHz range were tested in the GHz band. Susceptibility was characterized either by a prescribed threshold change on the output voltage or on the timing jitter. Although no upset was observed, perturbation criteria were reached at discrete frequencies up to ≈ 12 GHz followed by a sudden decrease with no more occurrence up to the 40 GHz limit of the setup. Even if very low effects were always observed at high frequency [3], we decided to irradiate a commercial analog circuit with a millimeter-wave source operating at 60 GHz to evaluate its electromagnetic susceptibility. To the best of our knowledge, this has never been done before.

2. EXPERIMENTAL SETUP

The experimental arrangement is given in Fig. 1. The mm-wave source is a Gunn oscillator (Quinstar, QTM-602001SV) delivering 20 dBm at 60 GHz. This source can be switched on and off using a TTL signal whose frequency f_m is limited to 20 kHz. A 35 dB isolator of 1.3 dB insertion losses ensures a stable operation whatever the load. An open-ended rectangular WR15 waveguide of size $a \times b = 3.76 \times 1.88$ mm^2 radiates the signal onto the device under test (DUT). The available power for EMI is thus ≈ 75 mW. The relative 3D positioning of the waveguide above the circuit package is achieved via motorized stages. To overcome the relatively low power of the source, the DUT package is placed as close as possible, in the near-field, at typical distances 100 µm $\leqslant h \leqslant 2$ mm that are well below the $\lambda = 5$ mm wavelength.

With a near-field experiment, it is no more possible to calibrate the impinging E-field using a probe dipole antenna and a powermeter as in [2, 3] because the probe size is at least of the order of the
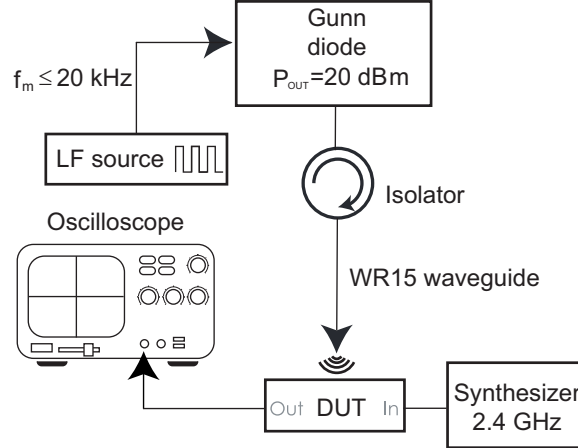
Figure 1. Scheme of the experimental setup.

wavelength. Alternatively, the E-field decrease with the distance has been quantified from theoretical estimations as follows. First the maximum transverse field E_{T_M} at waveguide center is obtained from the known power flowing through the waveguide by integrating the Poynting vector [4]

$$\mathcal{P} = \frac{E_{T_M}^2}{2}\sqrt{\frac{\epsilon_0}{\mu_0}}\sqrt{1 - \frac{\lambda^2}{4a^2}}ab,\tag{1}$$

yielding $E_{T_M} = 4.6\,\text{kV/m}$ with our $75\,\text{mW}$ source. The propagation of the transverse field $E_T(x,y,z)$ in free space is subsequently calculated using the method developed in [5], which results in the convolution the WR15 open-end $E_{T_0}(x,y)$ transverse field with a propagator

$$E_T(x,y,z) = -\frac{\partial G(r)}{\partial r} * E_{T_0}(x,y) \qquad \text{with} \qquad -\frac{\partial G(r)}{\partial r} = \frac{jk_0z}{2\pi r^2}e^{-jk_0r}\left(1 + \frac{1}{jk_0r}\right).\tag{2}$$

This has been done numerically, and both the maximum E-field along the z-axis and a complete profile at $z = 1\,\text{mm}$ are given in Fig. 2. A rapid decrease of the maximum field intensity is observed with distance, half of the initial value being reached as soon as $z = 1.35\,\text{mm}$.

In practice, it was not possible to move the open-end waveguide at distances smaller than $100\,\mu\text{m}$ because of the respective dimensions of the guide and of the circuit package and because of a risk of short-circuiting. Such a small h hereby guarantees that the maximum energy is transferred locally in
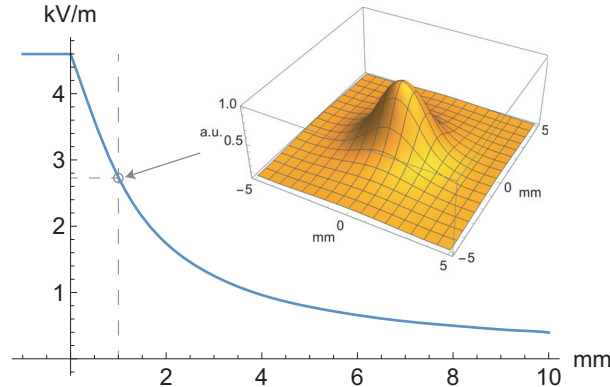

Figure 2. Calculated maximum intensity of the $60\,\text{GHz}$ transverse electric field radiated by the open-ended WR15 waveguide versus distance. Inset is a typical field profile calculated using Eq. (2) at the distance $h = 1\,\text{mm}$.

a small region of the circuit with a resulting EMI intensity in the range of a few kV/m. Such field intensities are of the same order of magnitude of what is usually produced by high-power microwave tests [3].

The DUT (Qorvo, RF6535) is a commercial front-end module that enables Wifi and Zigbee applications in the 2.4 GHz band. A switch is included to select either the transmit (TX) or receive path (RX). In TX mode, the power amplifier (PA) is selected and a typical 26 dB gain is achieved at the supply current $I_S = 72$ mA. In RX mode, the low noise amplifier (LNA) exhibits a typical 10.5 dB gain with $I_S = 10.7$ mA. Whatever the mode selected, the DUT is operated in the linear regime with a -20 dBm, $f_0 = 2.4$ GHz input signal obtained from a Keysight synthesizer N5171B. The output signal is monitored in the time domain using an Lecroy oscilloscope ZI610.

The circuit has a 500 µm thick package that brings an additional distance in between the IC surface, which is presumably the active receptor, and our mm-wave source. Such a distance is impossible to evaluate with accuracy without a destruction of the IC, but it is estimated to a few hundreds of micrometers on the basis of usual IC mounting procedures. In practice, this may have a noticeable influence on the EMI intensity if one refers to Fig. 2.

3. EXPERIMENTS

Preliminary experiments were conducted with the Gunn diode operated CW. PA and LNA were successively activated while the IC package was placed just below the waveguide. By monitoring the output of the selected function, a reduction in the amplitude of the 2.4 GHz signal was measured as a function of position and orientation owing to the motorized stages. Very close to the package at almost the minimum achievable distance $h = 100$ µm, we first searched for the maximum sensitivity position. When first activating the PA, a complete extinction was observed at the optimum EMI efficiency. Starting from that point, a $\pi/2$ rotation of the waveguide with respect to the IC makes the disturbance disappear. From these two observations, one then concludes that a 60 GHz field may perturb a common RF electronic device depending on its polarization and respective location. Furthermore, the amount of the disturbance is also dependent on the targeted function, PA or LNA, and does not necessarily occur at the same optimum location. In the sequel, the latter is called $M_{opt}^{function}$, and the ratio of the perturbed to unperturbed amplitudes is called the extinction ratio α_{CW} and quantified in percent. The amount of CW perturbation is reported in Fig. 3 where α_{CW} is plotted as a function of h for the most efficient polarization.

As evaluated previously in Fig. 2, the E-field intensity decreases by a factor 2.5 as a function of $h \in [0.1, 2]$ mm. Fig. 3 shows that both the PA and LNA are affected in that range because α_{CW} is zero at great distances and suddenly undergoes an important increase at a specific distance. For the three cases considered here, PA and LNA at M_{opt}^{PA} and LNA at M_{opt}^{LNA}, such thresholds occur at $h = 0.55, 0.79$ and 1.06 mm, which convert respectively to 3.50, 3.06 and 2.65 kV/m with the help of Fig. 2. Beyond that threshold, both PA and LNA outputs are attenuated by almost 50% over a wide h-range. For PA,
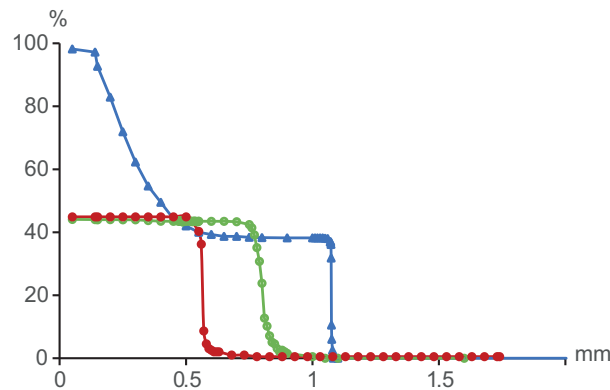

Figure 3. CW extinction ratio α_{CW} *vs* h. ▲: PA at M_{opt}^{PA}, ○: LNA at M_{opt}^{LNA}, ●: LNA at M_{opt}^{PA}.

α_{CW} increases further up to $\approx 100\%$ when h is reduced and copies almost perfectly the field increase when distance diminishes. This is not observed for the LNA, which shows a maximum perturbation of $\approx 45\%$ for the two positions considered. Notice that these two measurement points, $M_{\mathrm{opt}}^{\mathrm{PA}}$ and $M_{\mathrm{opt}}^{\mathrm{LNA}}$, were separated by $\approx 300\,\mu\mathrm{m}$, the possible distance separating the implantation of both functions on the die. Outcomes of CW tests are first the proof of a local perturbation of an IC by a near-field $60\,\mathrm{GHz}$ EMI injection with a spatial resolution which goes to the *inside of the IC*, and second a higher sensitivity of the PA to such EMI attack as compared to the LNA for the sample considered here.

In a second time the TTL chopper was applied to the Gunn diode, and the output of the Front-End was observed on the sampling scope. Fig. 4 shows the LNA output at $h = 100\,\mu\mathrm{m}$ and $f_m = 20\,\mathrm{kHz}$, the Gunn diode being active when the TTL control voltage is zero. The LNA output that appears as shaded areas, because the scope is triggered on the chopping signal, exhibits very strong variations which mimic the chopper with an extinction ratio almost complete when the $60\,\mathrm{GHz}$ EMI is applied. Notice that for the same conditions in CW mode, we had only $\alpha_{\mathrm{CW}} \approx 45\%$. The chopper, even if it is at very low frequency compared to both f_0 and the Front-End bandwidth, considerably enforces the perturbation. The underlying mechanism has yet to be elucidated.
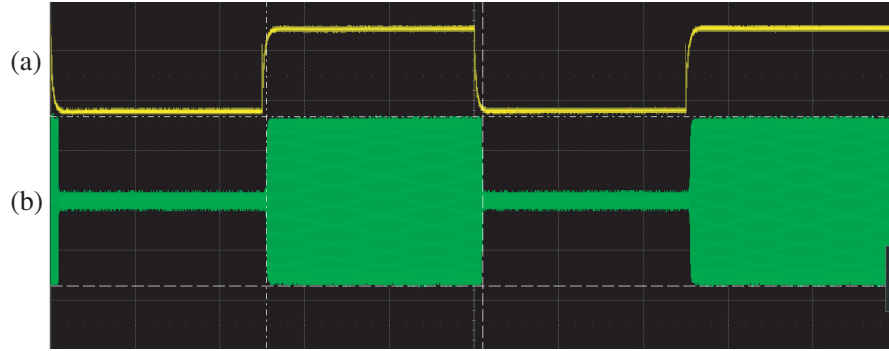

Figure 4. (a) TTL Gunn control voltage at $f_m = 20\,\mathrm{kHz}$. (b) LNA output under chopped mode at position $M_{\mathrm{opt}}^{\mathrm{LNA}}$ and $h = 100\,\mu\mathrm{m}$.

Fig. 5 shows PA outputs at the three heights $h = 100, 1100$ and $1200\,\mu\mathrm{m}$. The complete switching of the output signal at $h = 100\,\mu\mathrm{m}$ follows exactly the control, and this is not surprising since we already measured $\alpha_{\mathrm{CW}} = 100\%$ in CW mode at that height. The two other traces (Figs. 5c and 5d) correspond however to points where we had $\alpha_{\mathrm{CW}} \approx 20\%$ and $\alpha_{\mathrm{CW}} \approx 0\%$, respectively. The temporal evolution in chopped mode does not strictly reproduce the $60\,\mathrm{GHz}$ Gunn output. A sudden complete extinction of the function just follows the rising edge of the source, and then one observes a slow trumpet-shape recovery toward the $2.4\,\mathrm{GHz}$ amplitude given by α_{CW}. This dynamical behavior is here particularly evidenced by the choice of low f_m-values for each h allowing to recover the steady-state. It allows to define the recovery time τ_R as the time to recover 50% of the level reached in CW (see drawings in Fig. 5). Notice that in Fig. 4 we chose a high f_m with aim to show a possible complete extinction with the LNA. Nevertheless, a lower f_m would also have get this function recovery up to the $\alpha_{\mathrm{CW}} = 45\%$ value corresponding to experimental conditions.

The EMI attack dynamic is characterized by the recovery time τ_R whose determination from oscillograms is drawn for a non-zero α_{CW} in Fig. 5(c) and for $\alpha_{\mathrm{CW}} = 0$ in Fig. 5(d). Fig. 6 plots τ_R as a function of h for both the PA and LNA. The higher τ_R is, the more efficient the perturbation is, because the target is affected on a longer timescale. For instance, with the LNA, τ_R decreases from $1\,\mathrm{ms}$ at $h = 100\,\mu\mathrm{m}$ to a few $\mu\mathrm{s}$ at $h = 1.5\,\mathrm{mm}$, so even a square pulsed injection at $f_m = 1\,\mathrm{MHz}$ will remotely disable the LNA half the time at the latter distance. The effect is far more sensitive with the PA that recovers its function in almost $1\,\mathrm{ms}$ whatever $h \in [0.4, 1.1]\,\mathrm{mm}$. At shorter distances, τ_R could not be measured because it tends to infinity according to α_{CW} that increases up to 100%, and this is figured by a dashed line. On the other hand, with a sufficiently high f_m modulation, Fig. 6 shows that the PA can be significantly perturbed by our very moderate power source up to a distance exceeding $2\,\mathrm{mm}$.
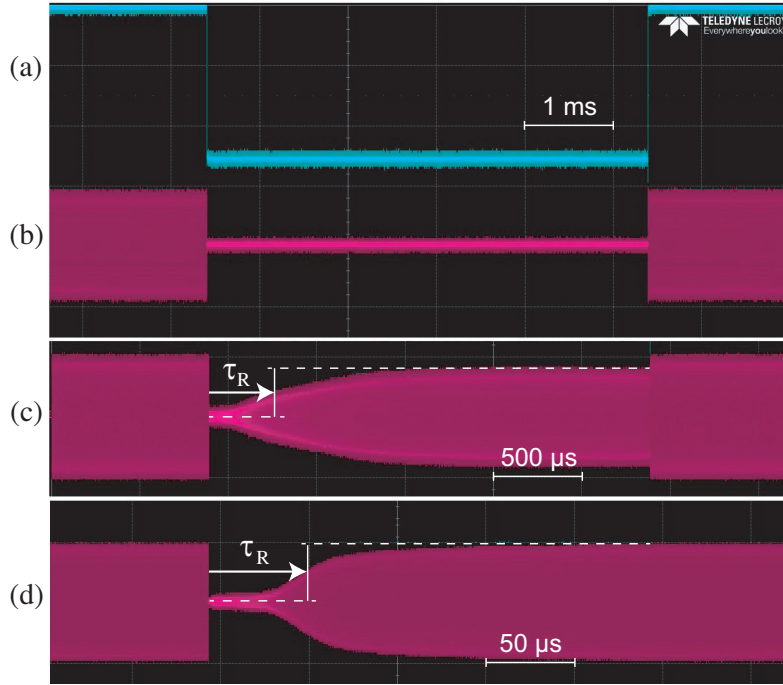
Figure 5. PA output under chopped mode at position $M_{\mathrm{opt}}^{\mathrm{PA}}$. X-axis is stretched so as every square pulse is of the same size whatever f_m. (a) TTL Gunn control voltage. (b) $h = 100\,\mu\mathrm{m}$. (c) $h = 1100\,\mu\mathrm{m}$. (d) $h = 1200\,\mu\mathrm{m}$.
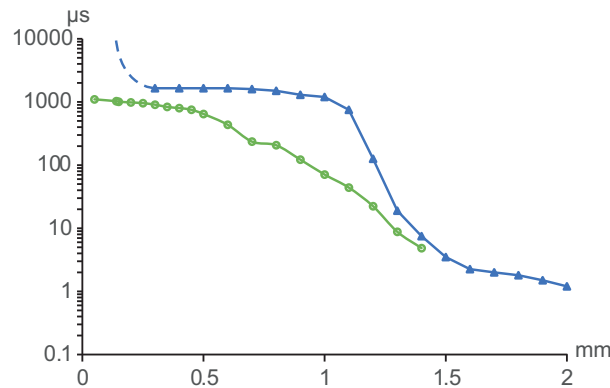

Figure 6. Recovery time τ_R *vs* h after the beginning of a pulsed aggression. ▲: PA, ○: LNA.

4. DISCUSSION AND CONCLUSION

Experiments have illustrated the possible remote extinction of a 2.4 GHz front-end module using an EMI produced by an mm-wave Gunn diode. The efficiency of the perturbation is considerably enhanced with a chopped microwave signal. Both the LNA and PA have been aggressed, the sensitivity of the latter being higher with our sample. Despite this difference, the observation of dynamic recovery signals of each function are very similar. To our eyes and without any knowledge of the physical implantation on the die, this is the proof that attacks have induced effects of the same kind on the same type of targets, probably the supply voltage lines because of their large size and the proven sensitivity to polarization.

When we highlighted these effects for the first time, we were very surprised because they were not foreseen in the literature [2, 3]. In addition, it was quite astonishing that a Wifi module, otherwise known

as very robust towards an EMI attack [6], could be so easily upset. This is probably because of the strong out-of-band character of the attack performed at mm-waves for a GHz circuit. The study will be extended in the future to more samples addressing different operating bands. Nonetheless, the physical mechanisms involved are still unknown and will certainly be unveiled only with a perfect knowledge of the layout and thus a close collaboration with a founder.

REFERENCES

1. Ramdani, M., E. Sicard, A. Boyer, S. B. Dhia, J. J. Whalen, T. H. Hubing, M. Coenen, and O. Wada, "The electromagnetic compatibility of integrated circuits — Past, present, and future," *IEEE Trans. Electromagn. Compat.*, Vol. 51, No. 1, 78–100, 2009.

2. Perdriau, R., O. Maurice, S. Dubois, M. Ramdani, and E. Sicard, "Exploration of radiated electromagnetic immunity of integrated circuits up to 40 GHz," *Electron. Lett.*, Vol. 47, No. 10, 589–590, 2011.

3. Backstrom, M. G. and K. G. Lovstrand, "Susceptibility of electronic systems to high-power microwaves: Summary of test experience," *IEEE Trans. Electromagn. Compat.*, Vol. 46, No. 3, 396–403, 2004.

4. Jackson, J. D., *Electrodynamics*, Wiley Online Library, 1975.

5. Baudrand, H., J.-W. Tao, and J. Atechian, "Study of radiating properties of open-ended rectangular waveguides," *IEEE Trans. Antennas Propag.*, Vol. 36, No. 8, 1071–1077, 1988.

6. Palisek, L. and L. Suchy, "High power microwave effects on computer networks," *EMC Europe*, 18–21, IEEE, York, 2011.